ENGINEERING JOURNAL

Article

Crystallization of Lead Phosphate in Gel Systems

Oratai Saisa-ard and Kenneth J. Haller*

School of Chemistry, Institute of Science, Suranaree University of Technology, Nakhon Ratchasima 30000, Thailand
E-mail: ken.haller@gmail.com*

Abstract. Lead phosphate crystals were grown in agarose gel at room temperature. Nucleation and crystal growth rates were controlled by changing the density of the gel medium including pure and phosphate gel. Individual crystallites from the pure gel layer show equant habit while those from the PO_4^{3-} gel layer show plate-like habit. Vibrational spectra indicate that the PO_4^{3-} ion is distorted and its symmetry is lower than free ion symmetry. Powder diffraction patterns of the pure gel products show mixed phases of $PbHPO_4$, $Pb_3(PO_4)_2$, and $Pb_5(PO_4)_3OH$ (PbHAp) consistent with saturation index predictions obtained from the PHREEQC program. Formation of the microscopic crystalline products was accompanied by a decrease in pH from 8 (theoretical for all layers mixed) to 3 for all reactions studied, consistent with $PbHPO_4$ being the major product. PbHAp does not appear in the phosphate gel layer because of the higher Pb:P ratio required for the PbHAp phase relative to the $Pb_3(PO_4)_2$ phase. PbHAp crystals from the gel crystallization method are first reported in this work as microcrystalline product deposited on the surface of the dominant phase formed in the pure gel layer.

Keywords: Lead phosphate, gel crystallization.

This paper is based on the poster presentation at the German-Thai Symposium on Nanoscience and Nanotechnology 2011—Green Nanotechnology of the Future, GTSNN 2011, in Nakhon Ratchasima, Thailand, 13-16 September 2011.

1. Introduction

Crystallization in gels is attractive for study due to the simplicity of the technique and the effectiveness in growing single crystals with very high perfection that are difficult to grow by other techniques. It has been applied to the study of crystal formation in human-related system such as cholesterol stone, gall stones, and urinary calculi. Furthermore, it provides an ideal technique to study crystal deposition diseases, which could lead to better understanding of the cause of disease [1-3].

Lead phosphates are interesting materials due to their properties. Lead hydrogen phosphate ($PbHPO_4$) and lead nitrate phosphate ($Pb_2(NO_3)(PO_4)$) show dielectric, piezoelectric, and optical properties which are useful in transducers and memory devices. Trilead bis(phosphate) ($Pb_3(PO_4)_2$) is known as a ferroelastic material with a phase transition near 180 °C [4-5]. While several researchers [6-9] have reported the growth of $PbHPO_4$ and $Pb_2(NO_3)(PO_4)$ in silica hydrogel, tetramethoxysilane gel, cross-linked polyacylamide gel, agar gel, and gelatin, the appearance of small crystals of lead hydroxyapatite, $Pb_5(PO_4)_3(OH)$, (PbHAp), in the gel layers or on the surfaces of other lead phosphate products has not been reported. PbHAp is a material of biological interest because of the similarity to calcium hydroxyapatite, $Ca_5(PO_4)_3(OH)$, (CaHAp), the dominant component in mammalian hard tissues such as bones and teeth; about 69 wt% and 95 wt%, respectively [10]. The relationship of PbHAp to CaHAp and its link to bone diseases like osteoporosis make the crystallization and growth of these materials of interest.

This paper presents results of lead phosphate growth in agarose gel with varied density of the gel medium. The PHREEQC speciation program is first used in this work to calculate possible phases in the lead phosphate system supporting formation of PbHAp and other lead phosphate phases. The relationship between synthesis conditions and crystal phases of products, including the formation of PbHAp, are discussed based on the results obtained.

2. Experimental

2.1. Sample Preparation

Diffusion of two soluble compounds through the agarose gel was set for the crystal growth in tubes as illustrated schematically in Fig. 1. Crystalline products are obtained in the gel when the two reactants meet. Diammonium hydrogen phosphate, $(NH_4)_2HPO_4$, and lead(II) nitrate, $Pb(NO_3)_2$, were used as PO_4^{3-} and Pb^{2+} sources, respectively. Varied densities of phosphate gel (1.0, 1.3, 1.5, 1.7, and 2.0 % w/v of agarose) were prepared by dissolving agarose powder (Vivantis, molecular biology grade) in 20 mL DI water with stirring for 10 min at 100 °C to give clear solutions. Crystallization experiments were set in small test tubes (1.5 x 10 cm) by adding 3.0 mL of the appropriate hot gel solution to 2.5 mL of warm 0.6 M phosphate solution (Ajax Finechem, AR grade), adjusting pH to 10 with NaOH, and allowing the mixture to stand 20 min to cool to room temperature to gel. A second layer of pure gel (1.0, 1.5, and 2.0 % w/v) was created by adding 1.5 mL of pure gel solution on top of the PO_4^{3-} gel layer and allowing 20 min to set the pure gel layer, after which 2.5 mL of 1.0 M lead nitrate solution (Ajax Finechem, AR grade) at natural pH was added on top of the gel layers. All reactions were kept at room temperature for two weeks. CO_2 was purged from the lead solution by passing Ar gas through the solution for 5 min before transfer.
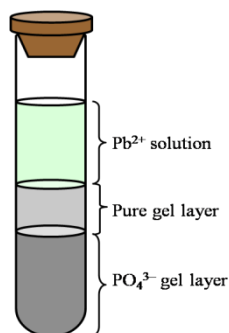

Fig. 1.   Experimental set up for gel crystallization of lead phosphate phases.

After two weeks the remaining solution was removed and the gel layers separated. Each gel layer was warmed to melt the gel and the solid products filtered off. The three solutions were combined and pH measured. The solids were washed with cold DI water and dried at 100 °C for 24 h.

2.2. Characterization

Crystal morphologies were observed by optical microscopy using an Olympus SZ40 microscope (Olympus, Japan) and scanning electron microscopy (SEM) using a JSM 6400 electron microscope (JEOL, Japan). IR spectra were acquired on a Perkin-Elmer model Spectrum GX Fourier transform infrared spectrophotometer (FTIR) in wave number range 400-4000 cm^{-1} from KBr pellets. Powder X-ray diffraction (XRD) scans were used for phase identification, 2θ range 10-60° using a Bruker axs D5005 diffractometer equipped with a Cu Kα X-ray source operating at 40 kV and 40 mA. The speciation program, PHREEQC V2 [11], with the *minteq.v4.dat* database [11] was used to calculate potential phase formation in the system assuming complete instantaneous mixing of the reactants.

3. Results and Discussion

Crystalline products were obtained inside both pure and PO_4^{3-} gel layers for all reactions as observed after two weeks reaction time. A typical result (density of phosphate and pure gel of 1.7 and 2.0 % w/v, respectively) is shown in Fig. 2.
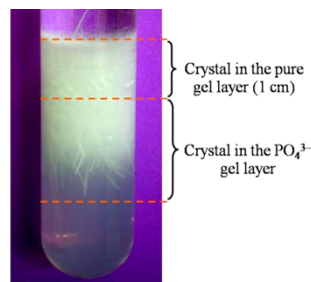

Fig. 2.   Crystalline products in pure and PO_4^{3-} gel layers for a typical reaction (see text).

Microscopic crystalline products were accompanied by a decrease in pH to 3 for all reactions studied. Their morphologies as observed by optical microscopy and SEM are illustrated in Fig 3.
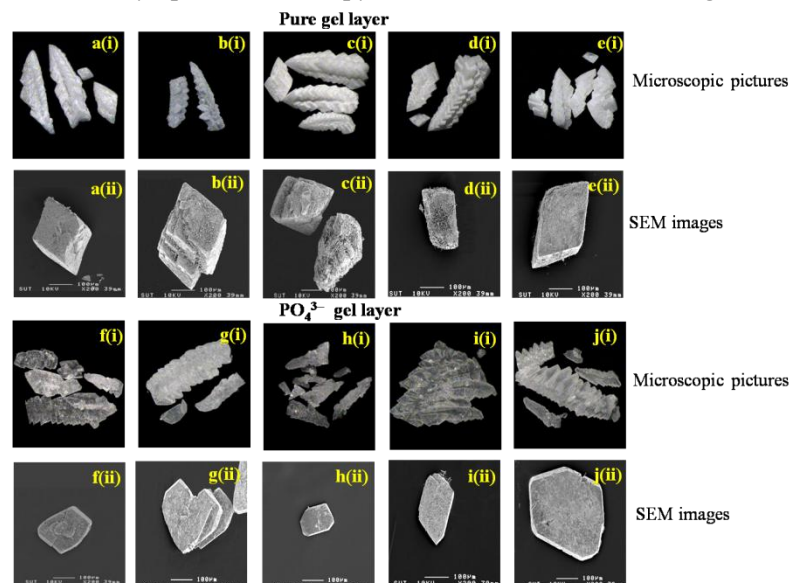

Fig. 3.   Microscopic pictures (2.5X) (i) and SEM images (ii) of products formed in the pure gel layer: (a-e) and PO_4^{3-} gel layer (f-j) with 2.0 % w/v of pure gel but different density of phosphate gel: (a) 1.0, (b) 1.3, (c) 1.5, (d) 1.7, (e) 2.0 % w/v.

Products appear as aggregates under optical microscopy in the pure gel layer (Fig. 3a(i)-e(i)) and in the PO_4^{3-} gel layer (Fig. 3f(i)-j(i)). Individual crystallites from the pure gel layer show equant habit (Fig. 3a(ii)-e(ii)), and those from the PO_4^{3-} gel layer show plate-like habit (Fig. 3f(ii)-j(ii)) as seen in low magnification SEM images.

Needle-like crystals with dimension about 2.5 x 10 μm are deposited on the surfaces of crystal products formed in the pure gel layer as can be seen in SEM images at higher magnification as shown in Fig. 4. These crystals have similar morphology to that reported by Mavropoulos *et al.* [12] for PbHAp. This observation further confirms that multiple product phases occur in this system, and indicates that they occur in sequential fashion. These small crystallites observed only in the pure gel layer occur for all the different densities of PO_4^{3-} gel layer.
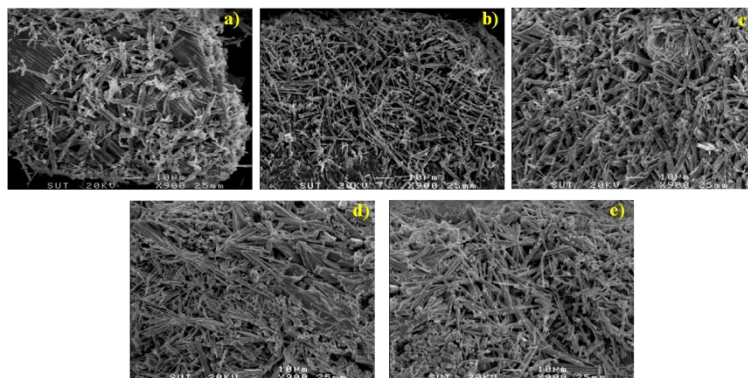

Fig. 4.   SEM images of crystal products obtained in the pure gel layer (2.0 % w/v), formed with different densities of PO_4^{3-} gel: (a) 1.0, (b) 1.3, (c) 1.5, (d) 1.7, (e) 2.0 % w/v.

IR wave number and assignments for the products are given in Table 1. All products give almost identical spectra that show characteristic bands of PO_4^{3-} group; bands in the regions 955-1046 cm^{-1}, 923-924 cm^{-1}, and 519-601 cm^{-1} reveal the asymmetric P–O stretching (υ_3), symmetric P–O stretching (υ_1), and O–P–O bending (υ_4), respectively.

Table 1.   IR frequencies (cm^{-1}) and assignments of crystal products from pure and phosphate gel layer.

Crystal in the pure gel layer	Crystal in the PO_4^{3-} gel layer	Assignment
~3555 w, b		($\upsilon_1 + \upsilon_3$) H_2O stretch
~1604 m		$\upsilon_2 H_2O$ bend
1384 vs		($\upsilon_1 + \upsilon_3$) NO_3, stretch
1348 vs		
1046 sh	~1100 s,b	$\upsilon_3 PO_4$ stretch
1004-1005 vs		
955-956 vs		
923-924 vs		$\upsilon_1 PO_4$, $\upsilon_1 HPO_4$ stretch
813-814 vw		$\upsilon_2 NO_3$ bend
715-716 vw		H_2O libration
705-706 vw		
600-601 m		$\upsilon_4 PO_4$ bend
539 m	548 s	
519-520 m		
398 sh	449 w	$\upsilon_2 PO_4$ bend,
	388 vw	$\upsilon_2 HPO_4$ bend

Abbreviations: w = weak, m = medium, s = strong, v = very, sh = shoulder, b = broad.

Assignments: υ_1 = symmetric stretching, υ_2 = bending, υ_3 = asymmetric stretching, υ_4 = bending.

An ideal PO_4^{3-} anion has tetrahedral point symmetry. Only absorptions corresponding to the υ_3 (955-1046 cm^{-1}) and υ_4 (519-601 cm^{-1}) vibrations should be observed. The υ_1 (923-924 cm^{-1}) and υ_2 (388-449 cm^{-1}) vibrations would be allowed in lower symmetry groups. The appearance of υ_1 and υ_2 in the IR spectra of both products from pure and PO_4^{3-} gel layers indicates the lower symmetry of PO_4^{3-} in the structure [13-14]. Water bending mode (1604 cm^{-1}) and O–H stretching mode (3555 cm^{-1}) are observed for the products obtained inside the pure gel layer but not for products obtained inside the PO_4^{3-} gel layer.

Bands at 1348-1384 and 813-814 cm^{-1} of products formed inside the pure gel layer which disappear after heating at 600 °C (Fig. 5) are assigned to residual nitrate from starting compound in agreement with previous work [15].
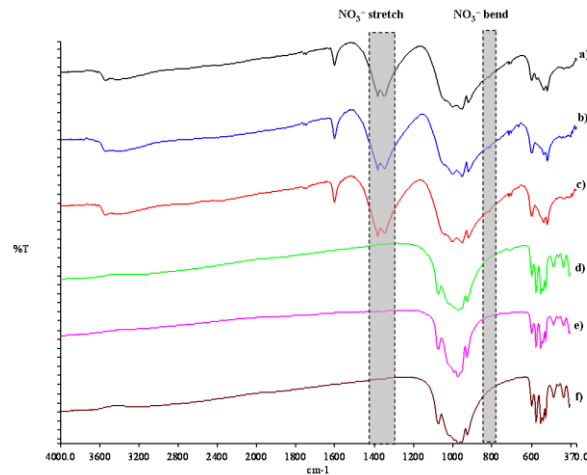

Fig. 5. IR spectra of products formed in the pure gel layer (2.0 % w/v) before heating; (a) 1.0, (b) 1.5, (c) 2.0 % w/v of PO_4^{3-} gel, and after heating at 600 °C; (d) 1.0, (e) 1.5, (f) 2.0 % w/v of PO_4^{3-} gel.

Search-match of the XRD patterns of crystal products obtained in the pure gel layer identify mixed phases containing PbHAp (JCPDS 1-0924), PbHPO$_4$ (JCPDS 6-0274), and Pb$_3$(PO$_4$)$_2$ (JCPDS 13-0278) as shown in Fig. 6(i) while products formed in the PO_4^{3-} gel layer show only peaks due to PbHPO$_4$ and Pb$_3$(PO$_4$)$_2$ (Fig. 6(ii)). Peaks due to PbHAp and Pb$_3$(PO$_4$)$_2$ phases are difficult to see because they are minor products. Small needle-like PbHAp crystals on the surface of products separated from the pure gel layer can be seen in the SEM images in Fig. 4. These results are consistent with predictions (assuming instantaneous mixing of all reactants in an aqueous solution) obtained from the PHREEQC program that calculates saturation indices based on aqueous solution activities for all species involved.
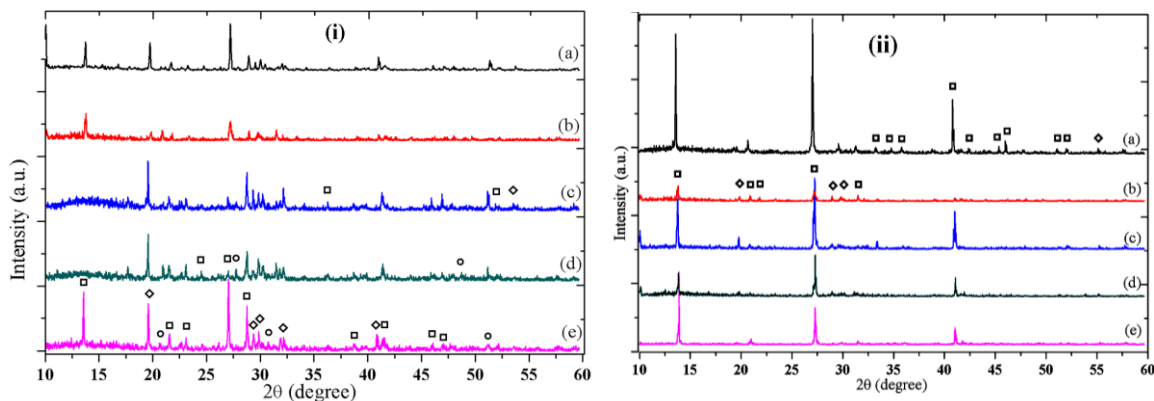

Fig. 6. XRD patterns of products obtained in the pure gel layer (i) and phosphate gel layer (ii) formed with 2.0 % w/v of pure gel and different densities of the phosphate gel: (a) 1.0, (b) 1.3, (c) 1.5, (d) 1.7, (e) 2.0 % w/v; (□) PbHPO$_4$, (◊) Pb$_3$(PO$_4$)$_2$, (○) PbHAp.

Saturation index (SI) uses calculated activities to provide a good indicator of the potential solid phases in a system at its equilibrium state [16]. SI is defined as Eq. (1):

$$SI = \log\left(\frac{IAP}{K_{sp}}\right) \qquad (1)$$

where IAP is the free ionic activity product and K_{sp} is the thermodynamic solubility product constant of a pure precipitate phase. SI relates to ΔG [17] as,

$$\Delta G = -2.303 RT \log\left(\frac{IAP}{K_{sp}}\right) \qquad (2)$$

where R is the ideal gas constant, and T is the temperature. From Eq. (2), ΔG equals zero when IAP = K_{sp} corresponding to SI = 0 and the solution is in equilibrium; ΔG is negative when IAP > K_{sp} corresponding to SI > 0; the solution is supersaturated and precipitation can occur (unless a metastable supersaturated solution occurs). However, ΔG is positive when IAP < K_{sp} corresponding to SI < 0 and the solution is undersaturated so precipitation cannot occur.

Calculation of SI requires detailed knowledge of the speciation of phosphate, lead compounds, and other related ions in the system. Speciation of relevant phosphate and lead compounds in the system is given in Table 2.

Table 2. Stability constants (K_a) for H_3PO_4 speciation, and solubility constants (K_{sp}) and saturation index (SI) for various lead compounds.

H_3PO_4 speciation	pK_a[a]	
$H_3PO_4 \rightleftharpoons H_2PO_4^- + H^+$	2.20	
$H_2PO_4^- \rightleftharpoons HPO_4^{2-} + H^+$	7.17	
$HPO_4^{2-} \rightleftharpoons PO_4^{3-} + H^+$	12.35	
Relevant lead compounds	pK_{sp}[b]	SI[c]
$Pb_5(PO_4)_3OH + 7H^+ \rightleftharpoons 5Pb^{2+} + 3H_2PO_4^- + H_2O$	62.79	13.17
$Pb_3(PO_4)_2 + 4H^+ \rightleftharpoons 3Pb^{2+} + 2H_2PO_4^-$	43.53	7.88
$PbHPO_4 \rightleftharpoons Pb^{2+} + HPO_4^{2-}$	23.80	2.08
$Pb(OH)_2 + 2H^+ \rightleftharpoons Pb^{2+} + 2H_2O$	−8.18	-0.48

[a] *Values from reference [16].*

[b] *Values from minteq.v4.dat database in reference [11].*

[c] *This work for the system described in the text.*

An initial pH = 10 in the PO_4^{3-} gel and initial pH of 6 in the 1M $Pb(NO_3)_2$ solution, imply a pH gradient through the "pure" gel layer from 10 to 6 as the reactants diffuse together (if all three layers were instantaneously mixed as an aqueous solution the pH would be 8). At pH = 10 the phosphate speciation (Fig. 7) predicts a small PO_4^{3-} concentration and HPO_4^{2-} as the dominant species. At pH = 6 $H_2PO_4^-$ is the dominant species with only a few percent HPO_4^{2-} and even less PO_4^{3-}. PHREEQC calculations based on the total initial concentrations of species in all layers combined indicate that $PbHPO_4$, $Pb_3(PO_4)_2$, and PbHAp would be supersaturated (pH = 8, and SI = 2.08, 7.88, and 13.17, respectively). The larger SI for the PO_4^{3-} containing species in spite of the low PO_4^{3-} concentration is a result of their solubilities being considerably lower than that of the HPO_4^{2-} containing species, and suggests they may nucleate first.

As phosphate ion is removed from the gel by precipitation, the speciation equilibrium will convert HPO_4^{2-} to H^+ and PO_4^{3-}, lowering the pH and at the same time adjusting the relative ion concentrations to favor HPO_4^{2-} until the hydrogen phosphate species nucleates. Of course if the hydrogen phosphate species nucleates first, the opposite logic applies until the phosphate compounds nucleate, but this would require two separate phosphate compounds to reach supersaturation and nucleate, which seems less probable. As growth proceeds, the trajectory of the pH will be determined by the relative sequestering of either or both phosphate or hydrogen phosphate in the solid phases.
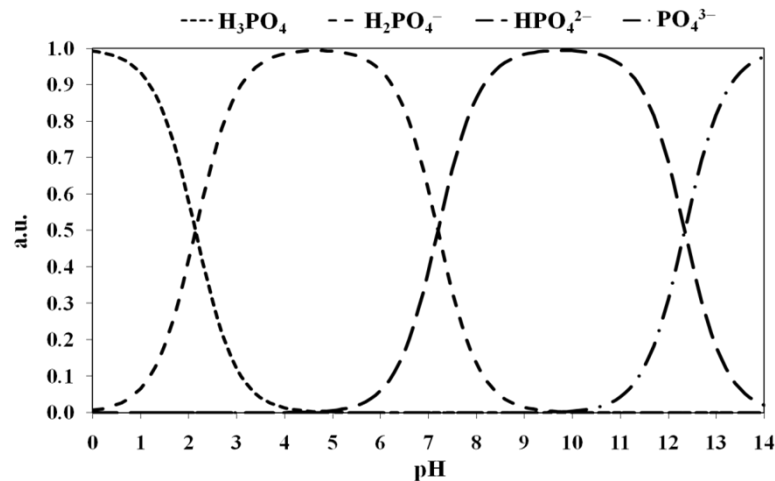
Fig. 7.   pH variation of ionic concentrations in the tripotic equilibrium for phosphoric acid solutions.

At the beginning of the experiment, the pH gradient in the pure gel layer is predisposed to higher pH by the procedure of placing the pure gel solution on the phosphate gel layer. Diffusion of ions from the phosphate layer will commence immediately, and a small amount of the phosphate gel will dissolve before the "pure" gel sets. Both effects favor increased PO_4^{3-} ion concentration near the lead solution, favouring initial precipitation of the phosphate phases in the pure gel layer. The presence of PbHAp in the pure gel layer but not in the phosphate layer can be understood based on the higher $Pb^{2+}:PO_4^{3-}$ ratio (5:3 vs. 3:2) required for the PbHAp phase relative to the $Pb_3(PO_4)_2$ phase.

4.   Conclusion

Speciation calculations indicate the possibility of forming mixed phases of $PbHPO_4$, $Pb_3(PO_4)_2$, and PbHAp in this system. XRD results confirm their formation, including the previously unreported gel precipitation of PbHAp. IR spectra of the crystalline products exhibit υ_1 and υ_2 vibrational bands indicating the lower point symmetry of PO_4^{3-} than tetrahedral. Formation of the microscopic crystalline products was accompanied by a decrease in pH from 8 (theoretical for all layers mixed) to 3 for all reactions studied, consistent with $PbHPO_4$ being the major product. Formation of $PbHPO_4$, $Pb_3(PO_4)_2$, and PbHAp phases with changing pH may be an important key for better understanding of the precipitation of biological hard tissues and the environmental geology of lead and phosphorus.

Acknowledgement

References

[1]   T. K. Anee, M. Palanichamy, M. Ashok, N. M. Sundaram, and S. N. Kalkura, "Influence of iron and temperature on the crystallization of calcium phosphates at the physiological pH," *Mater. Lett.*, vol. 58, pp. 478-482, 2004.
[2]   E. Ramachandran and S. Natarajan, "Crystal growth of some urinary stone constituents: II. In-vitro crystallization of hippuric acid," *Cryst. Res. Technol.*, vol. 37, pp. 1274-1279, 2002.
[3]   E. K. Girija, Y. Yokogawa, and F. Nagata, "Apatite formation on collagen fibrils in the presence of polyacrylic acid," *J. Mater. Sci.: Mater. Med.*, vol. 15, pp. 593-599, 2004.
[4]   D. M. C. Guimaraes, "Ferroelastic Transformations in lead orthophosphate and its structure as a function of temperature," *Acta Crystallogr. Sect. A*, vol. 35, pp. 108-114, 1979.
[5]   D. L. Decker, S. Petersen, and D. Debray, "Pressure-induced ferroelastic phase transition in $Pb_3(PO_4)_2$: A neutron-diffraction study," *Phys. Rev. B: Condens. Matter*, vol. 19, pp. 3552-3555, 1979.

[6] C. C. Desai and M. S. V. Ramana, "Nucleation density and electrolytic growth of lead hydrogen phosphate single crystals in silica gels," *J. Cryst. Growth*, vol. 102, pp. 191-196, 1990.

[7] C. C. Desai and M. S. V. Ramana, "Growth and properties of ferroelectric lead hydrogen phosphate and lead nitrate phosphate single crystals," *J. Cryst. Growth*, vol. 91, pp. 126-134, 1998.

[8] M. C. Robert and F. Lefaucheux, "A comparative study of gel grown and space grown lead hydrogen phosphate crystals," *J. Cryst. Growth*, vol. 88, pp. 499-510, 1988.

[9] B. Březina, M. Havránková, and K. Dušek, "The growth of $PbHPO_4$ and $Pb_4(NO_3)_2(PO_4)_2 \cdot 2H_2O$ in gels," *J. Cryst. Growth*, vol. 34, pp. 248-252, 1976.

[10] R. Z. LeGeros, "Calcium phosphates in enamel, dentin, and bone," in *Calcium Phosphates in Oral Biology and Medicine,* 1st ed. San Francisco, USA: Karger, 1991, ch. 6, pp. 110-111.

[11] D. L. Parkhurst and C. A. J. Appelo, *User's Guide to PHREEQC (version 2)-A Computer Program for Speciation, Batch-Reaction, One-Dimensional Transport, and Inverse Geochemical Calculations.* Denver, CO: U.S. Department of the Interior and U.S. Geological Survey, 1999.

[12] E. Mavropoulos, C. C. N. Rocha, C. J. Moreira, M. A. Rossi, and A. G. Soares, "Characterization of phase evolution during lead immobilization by synthetic hydroxyapatite," *Mater. Charact.*, vol. 53, pp. 71-78, 2004.

[13] V. M. Bhatnagar, "The preparation, x-ray and infrared spectra of lead apatites," *Archs. Oral Biol.*, vol.15, pp. 469-480, 1970.

[14] R. Ternane, M. Ferid, M. Trabelsi-Ayedi, and B. Piriou, "Vibrational spectra of lead alkali apatites $Pb_8M_2(PO_4)_6$ with M = Ag and Na," *Spectrochim. Acta, Part A,* vol. 55, pp. 1793-1797, 1999.

[15] A. A. Stepuk, A. G. Veresov, V. I. Putlyaev, and Yu. D. Tret'yakov, "The influence of NO_3^-, CH_3COO^-, and Cl^- ions on the morphology of calcium hydroxyapatite crystals," *Dokl. Akad. Nauk*, vol. 412, pp. 11-14, 2007.

[16] A. M. Ure and C. M. Davidson, "Predicting chemical speciation and computer simulation," in *Chemical Speciation in the Environment*, 1st ed. Glasgow, UK: Chapman and Hall, 1995, ch. 5, pp. 87-94.

[17] W. Stumm and J. J. Morgan, "The equilibrium constant," in *Aquatic Chemistry,* 3rd ed. New York, NY: John Wiley & Sons, 1996, ch. 2, pp. 41-43.